

## ESTIMATING THE TREHALOSE CYTOPLASMIC CONTENT DURING A BAKER'S YEAST PRODUCTION PROCESS

A. I. Cabrera, J. S. Aranda, J. I. Chairez

*Unidad Profesional Interdisciplinaria de Biotecnología del IPN  
Av. Acueducto S/N, Barrio La Laguna Ticomán, C. P. 07340  
México, D. F.*

**Abstract:** Trehalose is commonly used as an indicator of a good yeast fermentation capacity and viability. An attempt of estimating trehalose concentration in yeast cells through two different mathematical approaches is presented. It combines a biomass and trehalose concentrations estimator developed with a differential neural network technique, and a structured model applied for explaining the main metabolic events that induce trehalose accumulation. Our results allow us to think that the coupling of both methods can provide suitable information aimed at reaching a high trehalose content in an actual yeast production process.

*Copyright © 2007 IFAC*

**Keywords:** Yeast biomass, trehalose estimation, structured model, differential neural network, soft-biosensor.

### 1. INTRODUCTION

Cell viability and fermentation capacity (CO<sub>2</sub> production power) are probably the main properties determining yeast quality for its usage in both bread and alcoholic beverages making processes. Disaccharide trehalose is considered as a significant factor in preserving yeast viability (Attfield *et al.*, 1994; Lewis *et al.*, 1997; Weimken, 1990) and CO<sub>2</sub> release potential (Jørgensen *et al.*, 2002), because it determines in some extent the physiological condition and the biochemical composition of yeast cells. It has been shown that trehalose biosynthesis is induced by limiting the availability of carbon and nitrogen substrates in the extracellular medium (Parrou *et al.* 1999; Aranda *et al.* 2004; Eturgay *et al.*, 1997). Also, trehalose is an important parameter to be followed during the yeast biomass production process. Nevertheless, as this disaccharide is an intracellular compound, biomass samples must be

taken periodically to obtain the trehalose content in yeast through an off-line analytical technique. This means that intracellular trehalose concentration, and therefore yeast quality related to it, are known just after the yeast production process has been accomplished in time, only when it is no longer possible to opportunely apply correcting measures attempting to increase intracellular trehalose content at some stage of the yeast biomass production process. In order to avoid delayed quantification and to have some knowledge of cytoplasmic trehalose concentration during yeast production, a strategy for estimating trehalose content on-line is developed in this work. It consists of coupling a biochemically structured model for yeast growth and trehalose prediction, with a differential neural network structure aiming at generating very precise real-time estimations of intracellular trehalose and total biomass concentration as well.

### 1.1 Structured model description

The structured model considers the trehalose-enriched yeast production process depicted by three

Table 1 Structured model equations

| Abiotic states  | Physical meaning  |      |
|---|---|------|
| $\frac{dx}{dt} = \left(\mu - \frac{f_v}{v}\right)x$       | Biomass accumulation in the bioreactor                        | (1)  |
| $\frac{dv}{dt} = f_v$                                     | Variation of liquide volume in the bioreactor                 | (2)  |
| Biotic states   | Physical meaning  |      |
| $\frac{dw_T}{dt} = q_{ST} - q_{HT} - \mu w_T$             | Variation of intracellular mass fraction of trehalose         | (3)  |
| $\frac{dE_{TS}}{dt} = q_{ES} - q_{PS} - \mu E_{TS}$       | Variation of intracellular mass fraction of trehalose syntase | (4)  |
| $\frac{dE_{TH}}{dt} = q_{EH} - q_{PH} - \mu E_{TH}$       | Variation of intracellular mass fraction of trehalase         | (5)  |
| $\frac{d(cAMP)}{dt} = q_A - \mu(cAMP)$                    | Variation of intracellular concentration of cAMP              | (6)  |
| Kinetic equations   | Physical meaning  |      |
| $q_s = \frac{f_v}{vX} s_0$                                | Substrate consumption specific rate                           | (7)  |
| $\mu = Y_x q_s$   | Growth specific rate  | (8)  |
| $q_{ST} = k_S E_S$  | Intrinsic specific rate of trehalose synthesis                | (9)  |
| $E_S = \frac{E_{TS}}{k_{eq}[cAMP]^2 + 1}$                 | Trehalos syntase complex mass fraction (active conformation)  | (10) |
| $q_{HT} = k_H E_H$  | Intrinsic specific rate of trehalose hydrolysis               | (11) |
| $E_H = \frac{k_{eqH}[E_{TH}][cAMP]}{k_{eqA}[cAMP] + 1}$   | Trehalase mass fraction (active conformation)                 | (12) |
| $q_{ES} = k_{ES}\mu + \frac{k_1[G_{TS}]}{k_{eqS}[R] + 1}$ | Intrinsic specific rate of trehalose syntase production       | (13) |
| $q_{EH} = k_{EH}\mu + \frac{k_2[G_{TH}]}{k_{eqH}[R] + 1}$ | Intrinsic specific rate of trehalase synthesis                | (14) |
| $R = k_{eqR}[ApoR][cAMP]$                                 | Intracellular concentrtrion of repressor                      | (15) |
| $q_A = k_A q_s$   | Specific rate of intracellular cAMP synthesis                 | (16) |
| $q_{PS} = k_{PS} E_{TS}$                                  | Specific rate of trehalose syntase proteolysis                | (17) |
| $q_{PH} = k_{PH} E_{TH}$                                  | Specific rate of trehalase proteolysis                        | (18) |

abiotic variables or states (biomass concentration, substrate concentration and culture medium volume in the bioreactor) and four main biotic components (trehalose concentration in the cell, trehalose phosphate synthase activity, trehalase activity and cAMP intracellular concentration). Process evolution

of biotic and abiotic states is described by differential eqs. (1-6) included in Table 1. Note that as fermentation processes were carried out at substrate limiting conditions ( $s \approx 0$ ), the balance for substrate gives ecuation (7) in Table 1. This set of equations is coupled to the reported kinetic equations, and solved with the corresponding initial conditions and model parameters. A detailed explanation of the structured model is given in Aranda *et al.* (2004).

### 1.2 Biomass estimator and trehalose content observer based on differential neural networks

To estimate the process abiotic states, together with intracellular trehalose concentration, a dynamic neuro network observer (DNNO) is suggested in spite of the Kalman Filter techniques (Catlin, 1989; Zarchan and Musoff, 2000) because the objective in our case is about estimating the states evolution, not the parameters into the model. Under heavy uncertainty conditions, the DNNO offers significant potential advantages comparing to other identification and control techniques. In this study we have built a DNNO that incorporates a switching type term to correct current state estimates using only available data. The proposed DNNO is basically covered by the following ordinary differential equation:

$$\begin{aligned} \frac{d\hat{x}_i}{dt} &= A\hat{x}_i + W_1\sigma(\hat{x}_i) + W_2\varphi(\hat{x}_i)\gamma(u_i) + K_1(y_i - \hat{y}_i) \\ &+ K_2SIGN(y_i - \hat{y}_i) \\ \hat{y}_i &= C\hat{x}_i \end{aligned} \quad (19)$$

Here,  $\hat{x}_i$  is the state vector of DNNO representing the current estimates of abiotic states and the observer prediction of intracellular trehalose content as well,  $\hat{y}_i$  is the output of DNNO corresponding the estimates of measurable abiotic states,  $A$ ,  $K_1$  and  $K_2$  are constant matrices obtained from DNNO training by using the trial and error test with  $K_1$  being a linear proportional (Luenberger) correction term matrix, and  $K_2$  a sliding mode correction term matrix,  $\sigma(\cdot)$  and  $\varphi(\cdot)$  are standard sigmoid functions,  $\gamma(u_i)$  is the control function applied to the DNNO,  $C$  is an output formatting function and the sign function is given by:

$$SIGN(v) := (\text{sign}(v_1), \dots, \text{sign}(v_n)) \quad (20)$$

with,

$$\text{sign}(z) := \begin{cases} 1 & \text{if } z > 0 \\ -1 & \text{if } z < 0 \\ \text{not defined} & \text{if } z = 0 \end{cases} \quad (21)$$

Specifying the  $x_i$  and  $\hat{y}_i$  vector components would produce the following straightforward equivalences:  $x_1$  is the biomass concentration variation in the culture medium (abiotic state),  $x_2$  is the substrate concentration variation in the fermentation (abiotic state),  $x_3$  is the working volume in the bioreactor (abiotic state), and  $\hat{x}_4$  is the intracellular trehalose content estimate (biotic variable). The measurable data are two abiotic states,

consequently  $\hat{y}_2$  is the output substrate concentration estimate, and  $\hat{y}_3$  is the output liquid volume estimate in the bioreactor. Therefore,

$$y_t = [0 \quad x_2 \quad x_3 \quad 0] \quad (22)$$

Also in this case,

$$C = \text{diag}[0 \quad 1 \quad 1 \quad 0] \quad (23)$$

The estimated states are the biomass concentration and the intracellular trehalose content.

### 1.3 DNNO Training method

The weight matrix  $W_i$  ( $i=1,2$ ) is the output tuning by a special on-line learning procedure (Poznyak *et al.*, 2001), this matrix is updated with a special learning law described by the equation:

$$\dot{W}_i = \Phi(W_i, \hat{x}_t, u_t, y_t | W^{(0)}) \quad (24)$$

This learning law is discretely denoted by:

$$\dot{W}_i^{(i,j)} = -k u_t S_t^{(i,j)} \text{sign}(\tilde{W}_i^{(i,j)}); i, j=1, n \quad (25)$$

where  $S_t$  is any matrix with the condition  $\text{tr}\{S_t\}=1$ , and:

$$\begin{aligned} u_t &= \left\| N_\delta P \tilde{W}_i^T \sigma(\hat{x}_t) \right\|_{\Pi}^2 + 2e_t^T C N_\delta P \tilde{W}_i^T \sigma(\hat{x}_t) \\ \Pi &= C^T \Lambda_\delta C + \delta \Lambda_\delta, \quad \tilde{W}_i = W_i - W^{(0)*} \\ e_t &= y_t - C \hat{x}_t, \quad N_\delta = (C^T C + \delta I)^{-1}, \delta > 0 \end{aligned} \quad (26)$$

The convergence properties for this algorithm can be found detailedly described in Poznyak *et al.* (2005). The matrix  $P$  is the positive solution for the algebraic Riccati equation given by:

$$P \tilde{A}^{(0)*} + (\tilde{A}^{(0)*})^T P + P R P + Q = 0 \quad (27)$$

To guarantee a small enough state estimation error the adequate parameters of DNNO (eq. 19) should be selected. The stationary parameters  $A$ ,  $K_1$ ,  $K_2$  may be tuned during the so-called training process, in this training we selected these parameters in order to accomplish certain conditions. First, the matrices  $A$  and  $K_1$  are selected to assure the stabilization on  $\tilde{A}^{(0)*}$ , this means that:

$$\tilde{A}^{(0)*} = (A + K_1 C) \quad (28)$$

is Hurwitz. Finally, if the pair  $(C, A)$  is observable, then the parameter  $K_2$  can be determined by:

$$K_2 = \alpha P^{-1} C^T, \quad \alpha > 0 \quad (29)$$

The weights  $W_i$ , ( $i=1, 2$ ) are quickly adjusted on-line by the special differential learning law given above. The training procedure may be conducted by using only experimental measurements as a correction criterium of DNNO parameters, as well as

for an adequate selection of the initial conditions in the applied learning procedure. The adequate learning of DNNO (eq. 25) provides a small enough upper bound (in an average sense) for the state estimation error  $\Delta_t = \hat{x}_t - x_t$ . Further details on learning-training procedures are given in Poznyak *et al.* (2001) and Poznyak *et al.* (2004).

## 2. MATERIALS AND METHODS

### 2.1 Microorganism

All experiments were carried out with a commercial baker's yeast obtained from the market. The microorganism was isolated in order to have a one-cell derived colony, and then identified as *Saccharomyces cerevisiae*. The strain was maintained on slants (glucose 20 g L<sup>-1</sup>, yeast extract 10 g L<sup>-1</sup>, agar-agar 20 g L<sup>-1</sup>) at 4 °C.

### 2.2 Fermentation medium

Fed-batch yeast production experiments were done on a chemically well-defined fermentation medium: glucose 50 g L<sup>-1</sup>, KH<sub>2</sub>PO<sub>4</sub> 7 g L<sup>-1</sup>, CaCl<sub>2</sub>·2H<sub>2</sub>O 0.25 g L<sup>-1</sup>, NaCl 0.5 g L<sup>-1</sup>, MgCl<sub>2</sub>·6H<sub>2</sub>O 6 g L<sup>-1</sup>, mineral solution 10 mL L<sup>-1</sup>, vitamins solution 10 mL L<sup>-1</sup>. Five hundred milliliters of mineral solution contain FeSO<sub>4</sub>·7H<sub>2</sub>O (278 mg), ZnSO<sub>4</sub>·7H<sub>2</sub>O (288 mg), CuSO<sub>4</sub>·5H<sub>2</sub>O (7.5 mg), Na<sub>2</sub>MoO<sub>4</sub>·2 H<sub>2</sub>O (25 mg), MnSO<sub>4</sub>·H<sub>2</sub>O (169 mg), H<sub>2</sub>SO<sub>4</sub> a few drops. Five hundred milliliters of vitamins solution are prepared with biotin (1.5 mg), calcium pantothenate (20 mg), inositol (125 mg), pyridoxine-HCl (25 mg), thiamine (50 mg).

### 2.3 Inoculum development

Inoculum was grown in a 1 L flask containing 500 mL of the synthetic medium at 30 °C and 150 rpm over 24 h. The 15 L bioreactor was inoculated with the obtained biomass and an early batch fermentation was carried out on 6 L of culture medium. The fed-batch cultivations were initiated after 10 h of the previously established batch process.

### 2.4 Experimental conditions

A 15 L bioreactor (Applikon Z81315 M607) was utilized for all fed-batch experiments. The experimental conditions were: temperature 30 °C, pH 5.0, air flow 450 L h<sup>-1</sup>, dissolved oxygen 10 % of saturation value (0.8 mgO<sub>2</sub> L<sup>-1</sup> ca). The culture pH was controlled with ammonia-water (20 % v/v) and this solution was the only nitrogen source. In the fed-batch part, the glucose flow to the bioreactor was a function of the respiratory quotient (RQ), as calculated from effluent gas composition data. The glucose concentration in the working liquid in the bioreactor was always kept near to zero in order to minimize ethanol production. Starving conditions on carbon or nitrogen source were imposed at the end of the culture (last three hours) for inducing intracellular trehalose accumulation.

## 2.5 Analytical methods

**Trehalose.** Samples of 20 mg dry yeast were extracted twice with 3 mL of 0.05 M trichloroacetic acid in continuous shaking during 40 min each time. Trehalose was then determined by anthrone method.

**Biomass.** The yeast growth was followed by correlating biomass dry weight to the optical density of the culture at 620 nm (Hitachi U-2000 spectrophotometer).

**Glucose.** The glucose was determined by an automatic glucose oxydase method (YSI 2700 Select).

## 2.6 Computational method

Based on experimental data from four different fed-batch cultures of *Saccharomyces cerevisiae* the DNNO (eq. 19) was trained, and then the neuro-observer was implemented to estimate the biomass and trehalose states.

## 3. RESULTS AND DISCUSSION

Substrate depletion, either carbon or nitrogen, at the final three hours of a yeast growth process produces an increase in cytoplasmic trehalose (see Fig. 1).

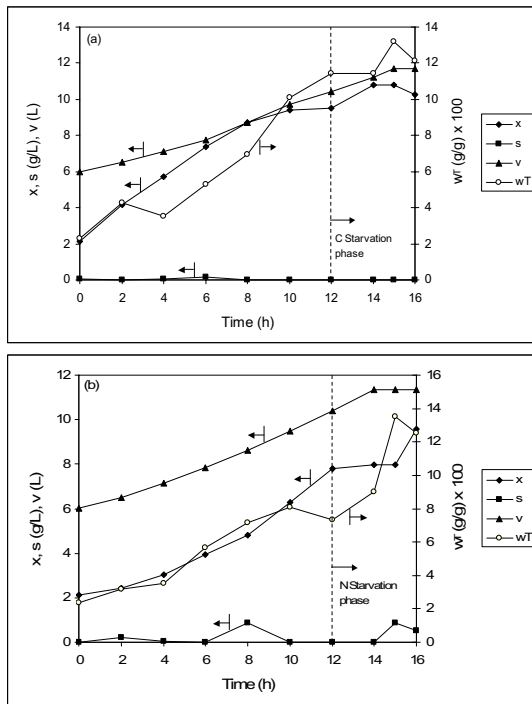


Figure 1. Biomass ( $x$ ), substrate ( $s$ ), intracellular trehalose ( $w_T$ ) and culture medium volume ( $v$ ) as functions of time during a yeast production process depleted in (a) carbon source and (b) nitrogen source, in the last three hours of the process.

Trehalose content in yeast cells was initially between  $0.025 - 0.035 \text{ g}_{\text{trehalose}} \text{ g}_{\text{biomass}}^{-1}$ , and intracellular accumulation of the disaccharide has reached a nearly 4-fold increase during the fed-batch

processes, attaining final concentrations of about  $0.13 \text{ g}_{\text{trehalose}} \text{ g}_{\text{biomass}}^{-1}$  (13 % of biomass dry weight) at the end of the culture.

A cascade of biochemical events after the substrate depletion explains the observed experimental trends of trehalose accumulation. Since the trehalose accumulation depends on the enzymatic activity of trehalase and trehalose phosphate synthase, and these enzymatic activities rely, in their turn, upon cAMP intracellular concentration, it can be assumed that nitrogen starvation produces an important modification of cAMP in the cell. The hypothesis is supported by reported evidence that adenylyl cyclase (the enzyme that catalyses the cAMP synthesis from ATP in the cell) is enhanced when a membrane associated Ras system is active. Like some other G-proteins, the activity of the Ras proteins is controlled by the guanine nucleotide, being inactive when bounded to GDP and active when it joins to GTP (Barbacid, 1987). While yeast is taken to a nitrogen-depleted culture medium, guanine nucleotides synthesis is stopped, and then the Ras system becomes inactive. As a consequence, cAMP synthesis could be stopped or, at least, decreased so giving low intracellular levels of cAMP. Similarly, a lack of glucose in the culture medium will produce a cytoplasmic shortage of adenosine phosphates, including cAMP. Under these conditions, trehalose phosphate synthase activity is increased with a concomitant lessening of trehalase activity, thus yielding a significant increment of trehalose in cells cytoplasm.

Table 2 Kinetic parameters for the structured model

| Model parameter | Numerical value      |                     |
|-----------------|----------------------|---------------------|
|                 | Limiting C           | Limiting N          |
| $f_v = f_v(t)$  | $0.11 \exp(0.08t)$   | $0.113 \exp(0.10t)$ |
| $Y_x$           | 0.43                 | 0.34                |
| $s_0$           | 45.1                 | 43.1                |
| $k_S$           | $1.4328 \pm 0.262$   |                     |
| $k_H$           | $0.5198 \pm 0.158$   |                     |
| $k_{ES}$        | $0.0156 \pm 0.0034$  |                     |
| $k_{EH}$        | $0.0218 \pm 0.0018$  |                     |
| $k_{eqS}$       | $2 \cdot 10^9$       |                     |
| $k_{eqH}$       | $2 \cdot 10^9$       |                     |
| $k_{eqR}$       | $0.1269 \pm 0.0127$  |                     |
| $k_A$           | $0.0023 \pm 0.00014$ |                     |
| $k_{eqI}$       | $0.01 \cdot 10^{-6}$ |                     |
| $k_{eqA}$       | $11.9483 \pm 2.309$  |                     |
| $k_I$           | $3.0650 \pm 0.240$   |                     |
| $k_2$           | $2.8327 \pm 0.194$   |                     |
| $k_{PS}$        | 0.09                 |                     |
| $k_{PH}$        | 0.07                 |                     |
| $G_{TH}$        | $4 \cdot 10^{-9}$    |                     |
| $G_{TS}$        | $4 \cdot 10^{-9}$    |                     |
| $ApoR$          | $2 \cdot 10^{-8}$    |                     |

Table 3 Initial conditions for model solution

| Limiting substrate | Initial conditions |         |             |                |                |                       |
|--------------------|--------------------|---------|-------------|----------------|----------------|-----------------------|
|                    | $x$ (g/L)          | $v$ (L) | $w_T$ (g/g) | $E_{TS}$ (g/g) | $E_{TH}$ (g/g) | $A$ ( $\mu\text{M}$ ) |
| Nitrogen           | 2,11               | 6,0     | 0,0237      | $10^{-4}$      | 0              | 5                     |
| Carbon             | 2,115              | 6,0     | 0,0232      | $10^{-4}$      | 0              | 5                     |

The main aspects of these physiological events have been captured in the structured model, so it is a useful tool to depict trehalose accumulation in yeast cells in a biomass production process (see Fig. 2).

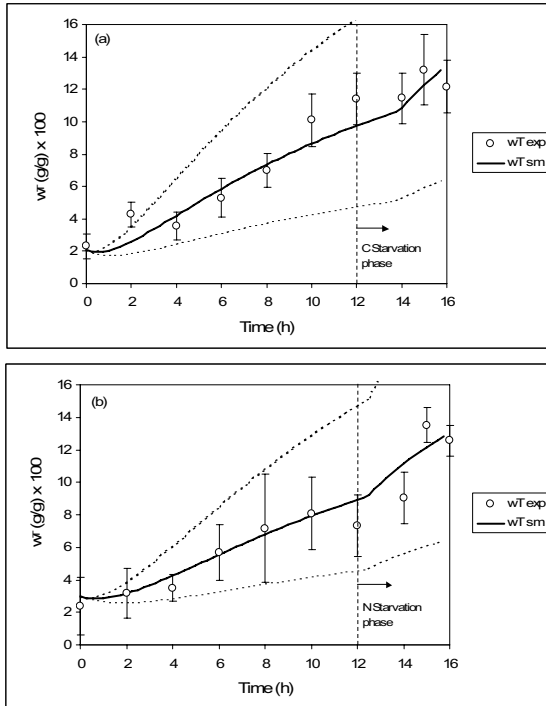


Figure 2. Intracellular trehalose content prediction in yeast cells through process simulation with a structured model, (a) carbon source starvation and (b) nitrogen source starvation. Empty marks are experimental measures, solid line is the model trend and dotted lines are upper and lower trehalose estimations within the parameters confidence intervals.

However, the accuracy of model predictions may not fulfill process simulation expectations because of the too large variations in the estimated yeast trehalose content. This accurateness problem won't allow to apply the appropriate correcting measures to shift a yeast production process towards the intended purpose of reaching a high intracellular trehalose concentration. The source of inaccuracy in the simulations is the lack of precision in parameters numerical values (see Table 2), and also the partial knowledge of the complex metabolic phenomena taking place in the yeast cells. The structured model is nevertheless helpful because it explains the biosynthesis intensification within the cells while the carbon or nitrogen substrates are exhausted in the culture medium.

Yeast production with a high intracellular trehalose needs a better forecast method for yeast trehalose content than the estimations given by a biochemically structured model. Another numerical estimations have been obtained by means of a DNNO algorithm. These estimates of biomass and intracellular trehalose concentrations, that were developed using the DNNO parameters of Table 4, are shown in Fig. 3 and Fig. 4. The DNNO real-time estimates approximated sufficiently well the

experimental states so the estimations are considered acceptably correct to depict the biomass evolution in the bioreactor (Fig. 3). However, the state evolution shows some oscillations that are due to the signum elements given in equation (25). This behaviour is not incorrect, but it can be improved by using a first order filter.

Table 4 DNNO parameter matrices obtained from training algorithms for each culture strategy (carbon or nitrogen limited yeast growth)

| Parameter | Yeast growth conditions   |   |
|-----------|---|---|
|           | Carbon limited growth   | Nitrogen limited growth   |
| $A$       | $\begin{bmatrix} -10.2 & 0 & 0 & 0 \\ 0 & -81 & 0 & 0 \\ 0 & 0 & -168.2 & 0 \\ 0 & 0 & 0 & -92.3 \end{bmatrix}$ | $\begin{bmatrix} -10.2 & 0 & 0 & 0 \\ 0 & -81 & 0 & 0 \\ 0 & 0 & -168.2 & 0 \\ 0 & 0 & 0 & -92.3 \end{bmatrix}$ |
| $K_1$     | $[1 \ 1 \ 100 \ 1]^T \times 0.01$   | $[1 \ 1 \ 100 \ 1]^T \times 0.01$   |
| $K_2$     | $diag[0 \ 0.0313 \ 0.0154 \ 0]$   | $diag[0 \ 0.0313 \ 0.0154 \ 0]$   |

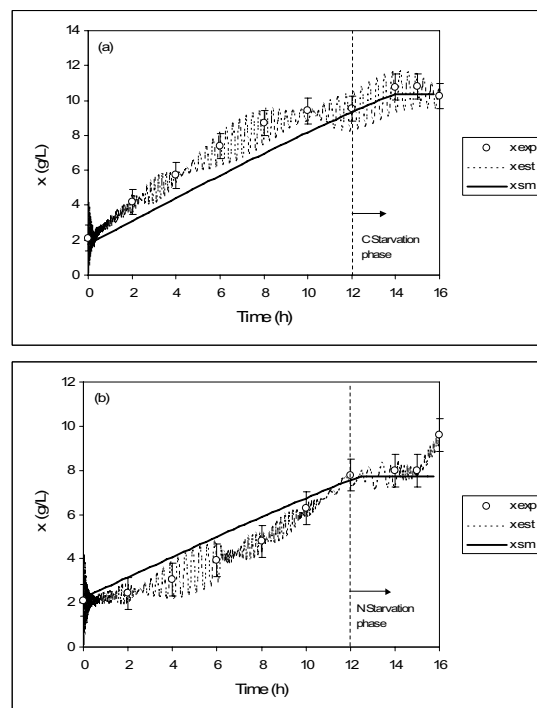


Figure 3. Estimation of biomass concentration in a yeast production process. Empty marks represent experimental values, dotted line is the DNNO estimations and solid line gives the numerical values of the structured model for (a) carbon-starved and (b) nitrogen-starved yeast cultures.

As shown in Fig. 4, DNNO intracellular trehalose estimations give a more regular behavior following the experimental results. These estimated values of trehalose content provide a more reliable basis for decision-making in production of yeast biomass with a high yield in cytoplasmic trehalose.

The presented trehalose and biomass estimator is based on the differential neural network theory applied to a fed-batch production process of *Saccharomyces cerevisiae*. The obtained results suggest the possibility of developing a new class of sensors called soft-biosensors.

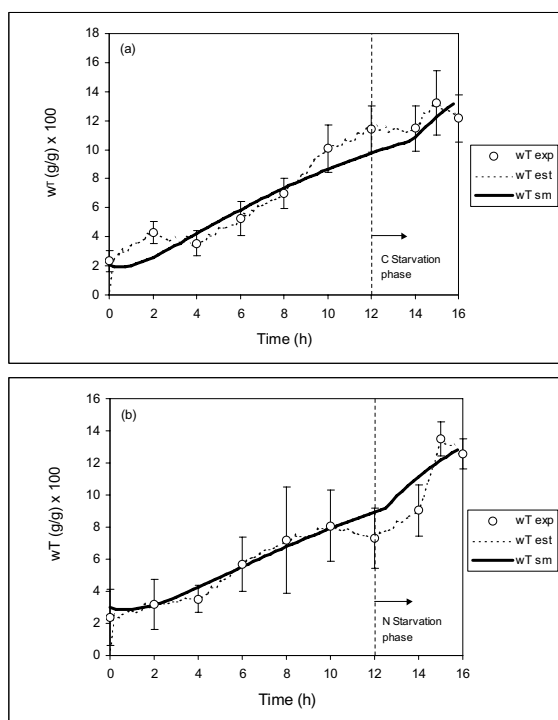


Figure 4. Intracellular trehalose content estimations in (a) carbon-starved and (b) nitrogen-starved yeast cultures. Empty marks refer to experimental data, dotted line represents the DNNO estimated values and solid line gives the structured model results.

#### 4. CONCLUSIONS

Intracellular trehalose predictions in yeast through a structured model and a DNNO technique provide complementary information about the process evolution. No possible physical meaning could be attached to a DNNO estimation, but these estimates of the trehalose accumulation dynamics are reliable enough to associate them to the proposed structured model in order to infer the cells metabolic condition regarding trehalose biosynthesis. The main proposal of this work is that by taking a DNNO intracellular trehalose content estimation, a metabolic state of the biomass can be conjectured by means of our structured model, because the estimated trehalose levels should correspond to certain standing of the metabolic fluxes in the biochemical pathways of the cell, including those of trehalose biosynthesis. Given an intracellular trehalose assessment, the enzymatic activity of trehalase (TH) and trehalose phosphate syntase (TPS) can be obtained by means of our structured model, and so the cAMP level within the cells, thus indirectly indicating the limiting source supply needed to continually produce a trehalose accumulation in cells while yeast production process

is taking place. An optimal planning and performing of a trehalose-enriched yeast production process should be accomplished by a suitable combined application of the two presented strategies for predicting trehalose content in *Saccharomyces cerevisiae* cells.

#### REFERENCES

- Aranda, J.S., E. Salgado and P. Taillandier (2004). Trehalose accumulation in *Saccharomyces cerevisiae* cells: experimental data and structured modeling. *Biochem. Eng. J.*, **17**, pp.129-140.
- Attfeld, P.V., S. Kletsas and B.W. Hazell (1994). Concomitant appearance of intrinsic thermotolerance and storage of trehalose in *Saccharomyces cerevisiae* during early respiratory phase of batch-culture is CIF1-dependent. *Microbiology*, **140**, pp. 2625-2632.
- Barbacid, M. (1987). Ras genes. *Annu. Rev. Biochem.*, **56**, pp. 779-827.
- Catlin, D. E. (1989). *Estimation, control, and the discrete Kalman filter*, Springer-Verlag, New York.
- Eturgay, N., H. Hamamci and A. Bayindirli (1997). Fed-batch cultivation of baker's yeast: effect of nutrient depletion and heat stress on cell composition. *Folia Microbiologica*, **42**, pp. 214-218.
- Jørgensen, H., L. Olsson, B. Rønnow and E.A. Palmqvist (2002). Fed-batch cultivation of baker's yeast followed by nitrogen or carbon starvation: effects on fermentative capacity and content of trehalose and glycogen. *Appl. Microbiol. Biotechnol.*, **59**, pp. 310-317.
- Lewis, J.G., R.P. Learmonth, P.V. Attfeld and K. Watson (1997). Stress cotolerance and trehalose content in baking strains of *Saccharomyces cerevisiae*. *J. Ind. Microbiol. Biotechnol.*, **18**, pp. 30-36.
- Parrou, J.L., B. Enjalbert, L. Plourde, A. Bauche, B. Gonzalez and J. François (1999). Dynamic responses of reserve carbohydrates metabolism under carbon and nitrogen limitations in *Saccharomyces cerevisiae*. *Yeast*, **15**, pp. 191-203.
- Poznyak, T.I., J.I. Chairez and A. Poznyak (2005). Application of a neural observer to phenols ozonation in water: Simulation and kinetic parameters identification. *Water Research*, **39**, pp. 2611-2620.
- Poznyak, A.S., E.N. Sanchez and W. Yu (2001). *Dynamic Neural Networks for Nonlinear Control: Identification, State Estimation and Trajectory Tracking*, World Scientific, New Jersey.
- Weimken, A. (1990). Trehalose in yeast, stress protectant rather than reserve carbohydrate. *A. van Leew. J. Microbiol.*, **58**, pp. 209-217.
- Zarchan, P. and H. Musoff (2000). *Fundamentals of Kalman filtering: a practical approach*, American Institute of Aeronautics and Astronautics, Reston Va.